Original Article

www.ToxicolRes.org
Toxicological Research

Toxicol. Res. Vol. 34, No. 2, pp. 133-141 (2018)
https://doi.org/10.5487/TR.2018.34.2.133

Open Access

Beneficial Effects of Cynaroside on Cisplatin-Induced Kidney Injury *In Vitro* and *In Vivo*

Jong-Hyun Nho[1,†], Ho-Kyung Jung[1,2,†], Mu-Jin Lee[1], Ji-Hun Jang[1], Mi-Ok Sim[1], Da-Eun Jeong[1], Hyun-Woo Cho[1] and Jong-Choon Kim[2]

[1]*National Development Institute of Korean Medicine, Jangheung, Korea*
[2]*College of Veterinary Medicine, Chonnam National University, Gwangju, Korea*

Abstract

Anti-cancer drugs such as cisplatin and doxorubicin are effectively used more than radiotherapy. Cisplatin is a chemotherapeutic drug, used for treatment of various forms of cancer. However, it has side effects such as ototoxicity and nephrotoxicity. Cisplatin-induced nephrotoxicity increases tubular damage and renal dysfunction. Consequently, we investigated the beneficial effect of cynaroside on cisplatin-induced kidney injury using HK-2 cell (human proximal tubule cell line) and an animal model. Results indicated that 10 μM cynaroside diminished cisplatin-induced apoptosis, mitochondrial dysfunction and caspase-3 activation, cisplatin-induced upregulation of caspase-3/MST-1 pathway decreased by treatment of cynaroside in HK-2 cells. To confirm the effect of cynaroside on cisplatin-induced kidney injury *in vivo*, we used cisplatin exposure animal model (20 mg/kg, balb/c mice, i.p., once a day for 3 days). Renal dysfunction, tubular damage and neutrophilia induced by cisplatin injection were decreased by cynaroside (10 mg/kg, i.p., once a day for 3 days). Results indicated that cynaroside decreased cisplatin-induced kidney injury *in vitro* and *in vivo*, and it could be used for improving cisplatin-induced side effects. However, further experiments are required regarding toxicity by high dose cynaroside and caspase-3/MST-1-linked signal transduction in the animal model.

***Key words*:** Cisplatin, Cynaroside, HK-2, Nephrotoxicity, MST-1

INTRODUCTION

Cynaroside is a flavone, a flavonoid-like compound. It is known under various names (Luteolin-7-*O*-glucoside, Luteoloside, Cinaroside), commonly found in *Lonicera japonica* Thunb. and *Angelica keiskei*. According to recent studies, cynaroside has absorbed in gastrointestinal tract, and it has an anti-oxidant effect, inhibiting lipid and protein oxidation (1-4). However, the protective effect of cynaroside on cisplatin-induced nephrotoxicity has not been elucidated.

Incidence of cancer mortality has increased with pollution and diet, despite development of medical standards and life (5). Cisplatin (*cis*-diamminedichloroplatium[II]) an anti-cancer drug, is commonly used in cancer treatment. However, despite wide use of cisplatin for cancer treatment, there are restrictions in using this anti-cancer drug because it may induce cardiotoxicity and nephrotoxicity (6). Cisplatin is eliminated from the body through filtration and secretions in kidneys, but it may cause nephrotoxicity if excessively used for cancer treatment (7-9). Thus, research on medicinal plants and active ingredients isolated from resource plants are needed for reducing negative side effects of chemotherapy.

MST (mammalian sterile 20-like kinase), a protein kinase (10), is involved in various cellular processes, such as transcriptional regulation, cell death, signal transduc-

Correspondence to: Hyun-Woo Cho, Tradition Korean Medicine Research Team, National Development Institute of Korean Medicine, 288, Jangheung 59338, Korea
E-mail: thej01234@gmail.com
Jong-Choon Kim, College of Veterinary Medicine, Chonnam National University, Gwangju 61186, Korea
E-mail: toxkim@jnu.ac.kr

[†]The first two authors contributed equally to this work.

pISSN: 1976-8257 eISSN: 2234-2753

tion, and post-translational modification (11,12). The MST protein family are common proteins expressed in almost all tissues. MST-1 was mostly expressed in kidneys. It was proteolytically activated caspase protein during apoptosis, and activated by apoptotic stimulation as well as other stress responses. MST-1 activation requires phosphorylation and caspase-3 mediated cleavage, resulting in autophosphorylation at Thr^{183} and Thr^{187} within its catalytic domain, leading to initiation of cell death including DNA fragmentation and chromatin condensation (13-15). Therefore, this study focused on the role of cynaroside under the condition of cisplatin exposure in HK-2 cell (human proximal tubule cell line). Thus, this study investigated 1) the relationship between cynaroside and caspase-3/MST-1 signal pathway in cisplatin-induced nephrotoxicity, 2) the protective effect of cynaroside on cisplatin-induced nephrotoxicity *in vivo* model.

MATERIALS AND METHODS

Chemicals. Cynaroside isolated from *Lonicera japonica* Thunb. (CAS 5373-11-5, purity: 97.5%) was purchased from Biopurify (Chengdu, Sichuan, China). Cisplatin (479306) and was purchased from Sigma Aldrich (St. Louis, MO, USA). Cisplatin fully dissolved in 0.9% NaCl, was stored at –20°C by protection from light.

Cell culture. HK-2 cells (human kidney proximal tubule cell) obtained from the Korean Cell Line Bank (KCLB, Seoul, Korea), were grown at 37°C in 5% CO_2 in Roswell Park Memorial Institute medium (RPMI 1640 medium) with 10% FBS (fetal bovine serum) and 1% penicillin/streptomycin. The media was changed every other day. Passaged cells were plated to yield near-confluent cultures at the end of experiments.

Animals. Male BALB/c mice (6 weeks of age) purchased from Samtako (Osan, Korea) were separated into 3 groups (Control; n = 7, Cisplatin; n = 7, Cisplatin + cynaroside; n = 7). Mice were administrated cisplatin (20 mg/kg, i.p., once a day, 3 days). After cisplatin administration for 30 min, cisplatin + cynaroside group was administrated with cynaroside (10 mg/kg, i.p., once a day, 3 days).

Measurement of cell viability. Cell viability measured by using Celliter 96® aqueous one solution cell proliferation assay (Promega, Fitchburg, WI, USA), according to manufacturer's instructions. Cells cultured in 96 well plate were incubated with various concentration of cynaroside (10, 20, 40, and 80 μM) or after treatment with 20 μM cisplatin for 30 min, HK-2 cells were treated with cynaroside (10, 20, 40, and 80 μM) for 24 hr. Cells were washed twice PBS (phosphate buffered salin) and treated with RPMI 1640 medium containing 20 μL MTS solution for 2 hr. Absorbance measured by using microplate reader infinite® PRO (TECAN, Mannedorf, Switzerland) at 490 nm. Relative cell viability (%) was expressed as percentage relative to the control group (non-treated group).

Tunel assay. Tunel assay was conducted using Dead-End™ fluorometric TUNEL system (Promega), according to manufacturer's instructions. HK-2 cells were seeded on cover glass in 12 well plate fixed in 10% NBF (neutralized buffered formalin) at 4°C for 20 min followed by permeabilization with 0.2% (v/v) Triton X-100 in PBS for 5 min, and washed with cold PBS for twice. Washed cells were used for Tunel assay. Paraffin sections were deparaffinized with xylene (Sigma Aldrich) and hydrated with water and diluted ethanol, and used for Tunel assay. Samples were incubated with equilibration buffer provided by kit for 5 min. After 5 min, samples were incubated with 100 μL rTdT incubation buffer at 37°C for 1 hr, and washed with 2X SSC buffer for twice. Samples were mounted with ProLing® glod antifade reagent with DAPI (Thermo, Waltham, MA, USA). Imaging was conducted on the epifluorescence microscope (Carl Zeiss, Oberkochen, Germany).

Protein extraction and Wes analysis. HK-2 cells were lysed in RIPA cell lysis buffer 2 (Enzo, Farmingdale, NY, USA) containing Pierce™ protease and phosphatase inhibitor mini tablets (Thermo) for 1 hr. Cell lysate was centrifuged for 10 min at 13,000 rpm at 4°C, protein levels were quantified using Bradford procedure. Whole cell lysate (1 μg) analyzed using Wes (Protein simple, CA, USA) according to manufacturer's instructions.

Caspase-3 activity assay. Caspase-3 activity assay conducted by using Caspase-3 colorimetric detection kit (Enzo), according to manufacturer's instructions. HK-2 cells were lysed in RIPA cell lysis buffer 2 (Enzo) containing Pierce™ protease and phosphatase inhibitor mini tablets (Thermo) for 1 hr. Cell lysate was centrifuged for 10 min at 13,000 rpm at 4°C, protein levels were quantified using Bradford procedure. Whole cell lysate (20 μg) used to caspase-3 activity assay.

Annexin-V/PI (propidium iodide) staining. Annexin-V/PI staining conducted with Annexin V-FITC apoptosis detection kit (Enzo) according to modified manufacturer's instructions. HK-2 cells cultured in 6 well plate were washed with cold PBS and then filled with 1 mL of Accutase (Innovative Cell Technologies, CA, USA). After 2 min, plate was carefully tapped to detach cells. Resuspended cells were washed twice with cold PBS and then resuspended in a binding buffer containing FITC-conjugated annexin V and PI. After 10 min at room temperature

in the dark, apoptotic cells were analyzed by CytoFLEX (Beckman Clulter, Indianapolis, IN, USA). FITC and PI double negative cells (LL; lower-left) were considered as normal cells. FITC-positive and PI-negative cells (LR; lower-right) were early apoptotic cells and FITC and PI double positive cells (UR; upper-right) were late apoptotic cells. FITC-positive and PI positive cells (UL; upper-left) were considered as necrosis. Apoptotic cell death was calculated by the sum of early apoptotic cells and late apoptotic cells (LR + UR).

JC-1 staining. HK-2 cells cultured in 6 well plates were incubated with 2 μM 5,5′,6,6′-tetrachloro-1,1′,3,3′-tetraethyl benzimidazolylcarbocyanine iodide (JC-1; Thermo) for 30 min. Cells were washed with cold PBS and then filled with fresh cold PBS. Stained cells were observed with the epi-fluorescence microscope (Carl Zeiss) under following fluorescence (JC-1 Monomer: Ex 485 and Em 530 nm, Aggregated JC-1: EX 535 and Em 590 nm). For flow cytometry analysis, washed cells were incubated with Accutase (Innovative Cell Technologies). After 2 min, plates were carefully tapped to detach cells. Resuspended cells were washed twice with cold PBS and then resuspended in cold PBS. Flow cytometry was used to quantify the JC-1 fluorescence. Lowered mitochondrial membrane potential is indicated by a switch to a decrease in red fluorescence accompanied with an increase in green fluorescence.

Blood cell analysis. Blood cells analysis conducted using IDEXX Procyte DX gematology analyzer (IDEXX, Westbrook, ME, USA) according to manufacturer's instructions. Whole blood was collected in BD Vactutainer™ glass blood collection tube with K_3 EDTA (Thermo), and used for blood cell analysis. Imaging was indicated lymphocyte (blue color), neutrophil (pink color), and monocyte (red color).

Blood chemistry analysis. Blood chemistry analysis conducted using FUJI DRI-CHEM 4000i (Fujifilm, Tokyo, Japan), according to manufacturer's instructions. Whole blood collected in BD Vacutainer™ SST tube (Thermo), incubated at room temperature for 10 min. Blood centrifuged for 10 min at 4,000 rpm at 4°C, separated serum samples were used for blood chemistry analysis (BUN, blood urine nitrogen; Cre, creatinine).

Hematoxylin & Eosin staining. Kidneys were harvested from mice, fixed in 10% NBF overnight and then paraffinized with paraffin, xylene, and diluted ethanol. Paraffinized kidney samples were cut into 4 μM using microtome (Leica, Wetzlar, Germany). Paraffin sections were deparaffinized with xylene (Sigma Aldrich) and hydrated with water and diluted ethanol, and used for hematoxylin & eosin staining.

Statistical analysis. Results were expressed as mean ± the SEM. Values are mean ± SEM of three independent experiments. For group comparisons, statistical analysis was conducted using one-way ANOVA by SPSS (SPSS Inc., IL, USA), followed by the Tukey post hoc test and Duncan's multiple rage test, were used. A value of $p < 0.05$ was considered significant.

RESULTS

Cynaroside treatment reduces cisplatin-induced cell death and DNA fragmentation in HK-2 cell. To confirm the protective effect of cynaroside in cisplatin-induced cell death, HK-2 cells (human proximal tubule cell) were pretreated with various concentrations (1.25, 2.5, 5, and 10 μM) for 30 min. After pre-treatment, cells were treated with 20 μM cisplatin for 24 hr. Cell viability was measured by MTS assay, HK-2 cell death was reduced by pretreatment of 5 and 10 μM cynaroside (Fig. 1A). As shown in Fig. 1A, cell viability significantly decreased by 20 μM cisplatin at 75.8 ± 1.0%, but recovered by 10 μM cynaroside at 86.6 ± 3.0%. Next, Tunel assay was conducted to reveal DNA fragmentation during the cell death process, visualized by Tunel assay (Fig. 1B). The Tunel positive

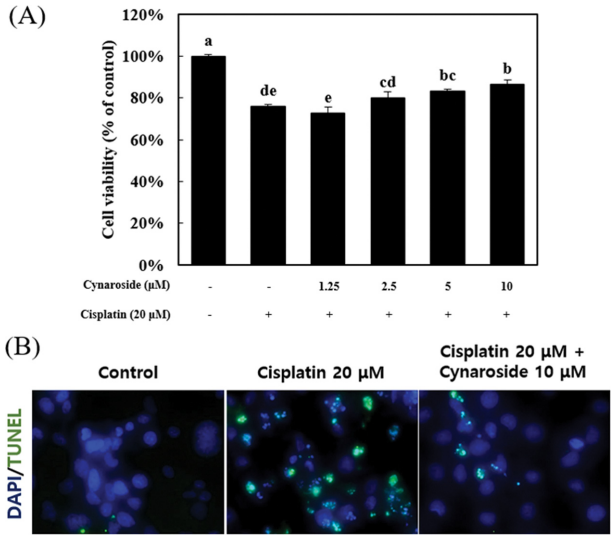

Fig. 1. Cynaroside prevents cisplatin-induced cell death in HK-2 cells. (A) HK-2 cells were treated with cynaroside for various concentration (1.25, 2.5, 5 and 10 μM). Cell viability was measured by MTS assay. Data represent the mean ± SEM of four independent experiments. (B) After pretreatment with 10 μM cynaroside, HK-2 cells were treated with 20 μM cisplatin for 24 hr. HK-2 cells were visualized by tunel assay. Representative images were taken from at least three independent experiments. *Means with difference letters are significantly different at $p < 0.05$ by Duncan's multiple range test.

signal increased by treatment of 20 μM cisplatin, but decreased by pre-treatment of 10 μM cynaroside. This result indicated that cisplatin-induced cell death was diminished by pre-treatment of 10 μM cynaroside in HK-2 cells.

Cynaroside treatment attenuates cisplatin-induced apoptosis and mitochondrial dysfunction in HK-2 cell. To reveal the inhibition effect of apoptosis and mitochondrial dysfunction during cell death, cells were pre-treated with 10 μM cynaroside for 30 min. After pre-treatment, cells were treated with 20 μM cisplatin for 24 hr. Apoptotic cell death was measured by Annexin V/PI staining. Under these condition, dysfunction of mitochondrial membrane potential (MMP) determined by JC-1 staining. As shown in Fig. 2A, apoptotic cell death increased by 20 μM cisplatin at 24.12 ± 2.6%. but was diminished by 10 μM cynaroside at 13.15 ± 2.4% (Fig. 2A). MMP is indicated by decrease in the red/green fluorescence intensity ratio, the green color shift is due to formation of red fluorescence J-aggregates. Results indicated that red fluorescence decreased by 20 μM cisplatin at 49.26 ± 5.8% than control group (red fluorescence; 76.41 ± 3.8%), and recovered by 10 μM cynaroside at 74.47 ± 3.5% (Fig. 2B). Collectively, apoptotic cell death and mitochondrial dysfunction were diminished by pre-treatment of cynaroside on cisplatin-induced cell death in HK-2 cell.

Cisplatin-induced caspase-3/MST-1 signal is attenuated by cynaroside treatment. Amin *et al*. (13) reported that MST-1 interacted with caspase-3 protein during apoptotic cell death in mammalian cell. It has also been reported that MST-1 is mostly expressed in kidney, closely associated with apoptotic cell death (11). In this study, 20 μM cisplatin treatment increased Caspase-3/MST-1 signaling pathway, decreased by pre-treatment with 10 μM cynaroside (Fig. 3A). Caspase-3 activity increased by 20 μM cisplatin at 134.40 ± 1.5% than the control group, but was diminished with pre-treatment of 10 μM cynaroside at 110.70 ± 2.9% (Fig. 3B). In summary, cisplatin-induced apoptosis via caspase-3/MST-1 signaling pathway and caspase-3 activation was abolished by cynaroside treatment, suggesting that cynaroside may be inhibited caspase-3/MST-1 signaling during cisplatin-induced cell death in HK-2 cell.

Effects of cynaroside on cisplatin-induced nephrotoxicity on blood analysis. To evaluate the protective effect of cynaroside on cisplatin-induced nephrotoxicity *in vivo*, we used the cisplatin nephrotoxicity model (20 mg/kg, balb/c mice, i.p., once a day for 3 days). In accordance with results from HK-2 cells, cisplatin administration increased blood neutrophils (Fig. 4A). BUN (blood urine nitrogen) and Cre (creatinine) in serum increased by cis-

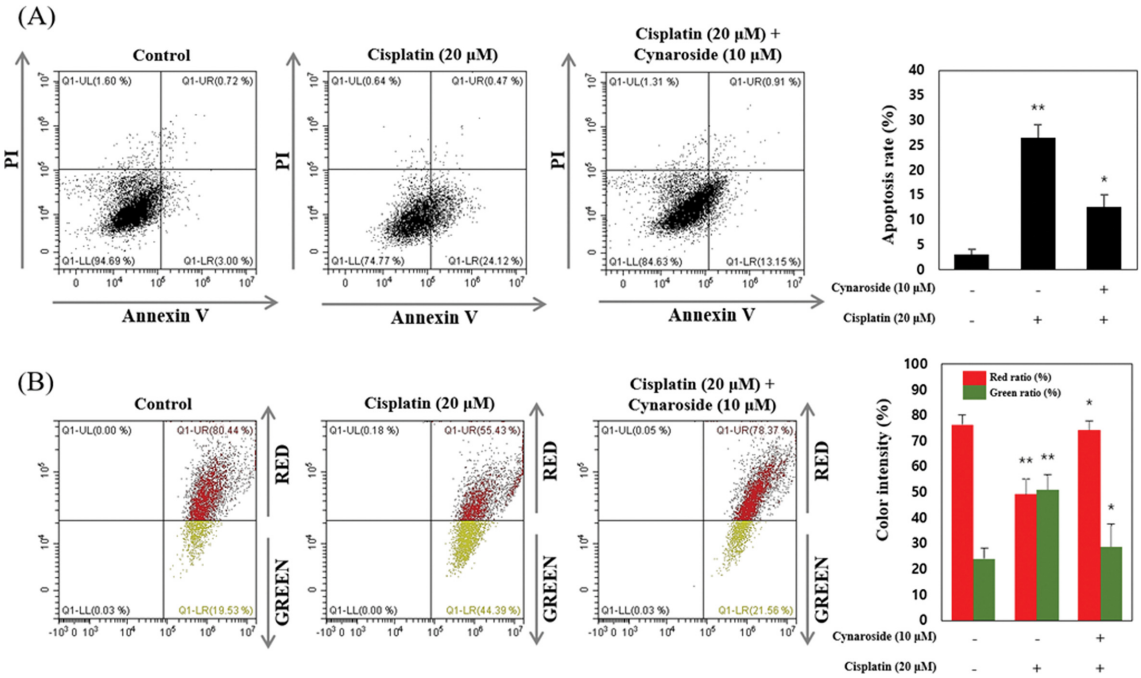

Fig. 2. Cynaroside reduces cisplatin-induced apoptosis and mitochondrial dysfunction in HK-2 cells. (A-B) After pretreatment with 10 μM cynaroside, HK-2 cells were treated with 20 μM cisplatin for 24 hr. Annexin V and propidium iodide staining and JC-1 staining were analyzed by flow cytometry. Data represent the mean ± SEM of three independent experiments. Representative images were taken from at least three independent experiments. *Means with difference letters are significantly different at $^{*}p < 0.05$ vs. cisplatin (20 μM), $^{**}p < 0.05$ vs. control.

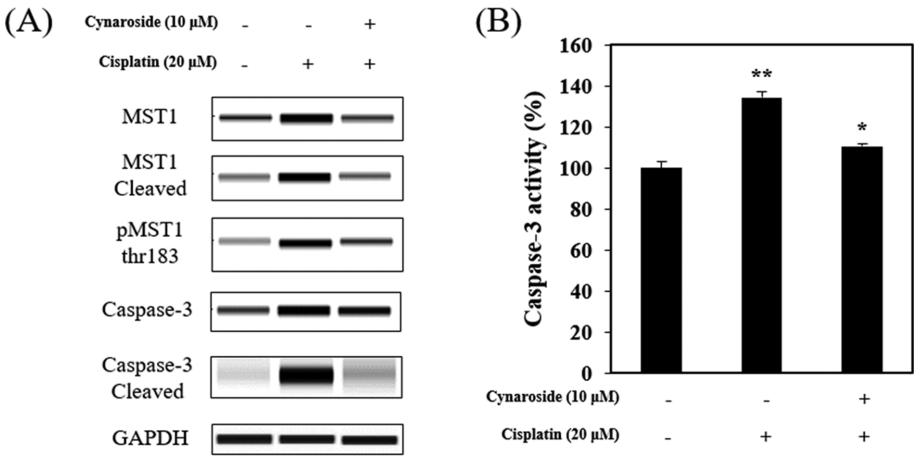

Fig. 3. Cynaroside reduces caspase-3/MST-1 signal pathway in HK-2 cells. (A-B) After pretreatment with 10 μM cynaroside, HK-2 cells were treated with 20 μM cisplatin for 24 hr. Cell extracts were subjected to protein analysis using wes and caspase-3 activity assay. Data represent the mean ± SEM of three independent experiments. Representative images were taken from at least three independent experiments. *Means with difference letters are significantly different at $^{*}p < 0.05$ vs. cisplatin (20 μM), $^{**}p < 0.05$ vs. control.

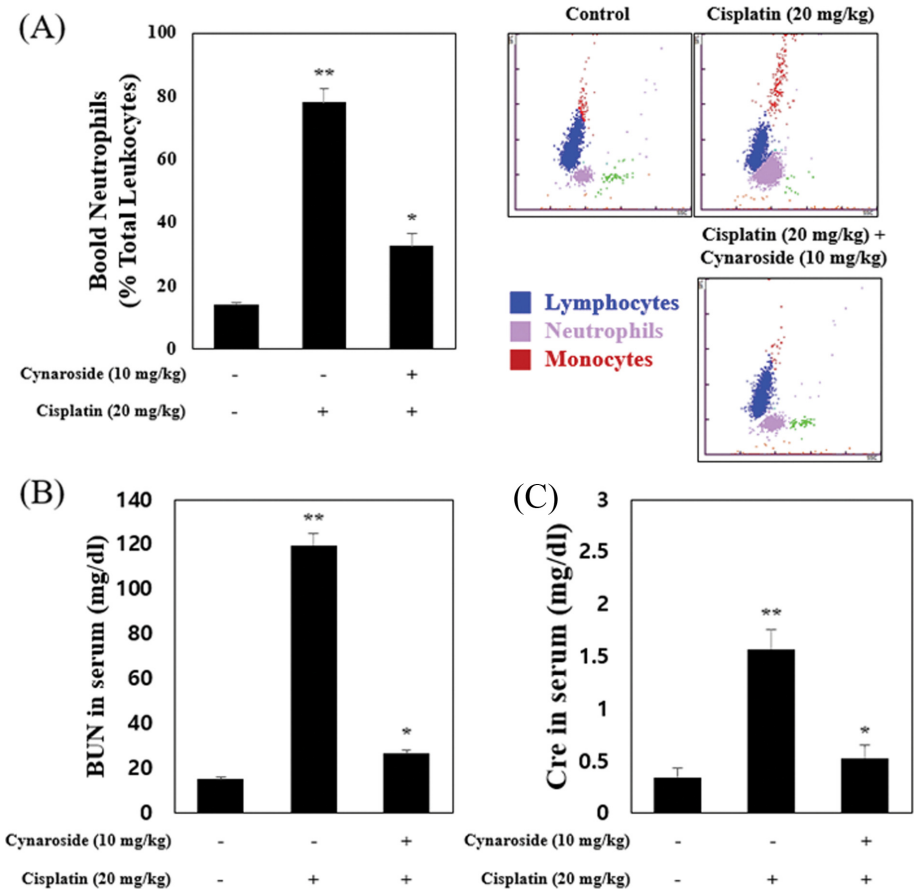

Fig. 4. Cynaroside reduces BUN, Cre and neutrophils in blood on cisplatin animal models. (A-B) Mice were separated 3 group (Control; n = 7, Cisplatin (20 mg/kg); n = 7, Cisplatin (20 mg/kg) + Cynaroside (10 mg/kg); n = 7). Mice were administered with vehicle or cisplatin (20 mg/kg). Blood neutrophils were analyzed by IDEXX procyte (A). BUN (B) and Cre (C) in serum are analyzed by FUGI DRI-CHEM 4000i. Data represent the mean ± SEM of three independent experiments. *Means with difference letters are significantly different at $^{*}p < 0.05$ vs. cisplatin (20 μM), $^{**}p < 0.05$ vs. control.

platin administration (Fig. 4B). As shown Fig. 4A, neutrophils in whole blood increased by cisplatin administration at 77.47 ± 4.6% on white blood cells than the control group (blood neutrophil; 14.12 ± 0.7%), and recovered by cynaroside administration at 32.72 ± 3.6% on white blood cells. Serum level of BUN and Cre increased by cisplatin administration (cisplatin group; BUN, 124.90 ± 5.2 mg/dL; Cre, 1.57 ± 0.1 mg/dL), and decreased by cynaroside administration (cisplatin + cynaroside group; BUN, 26.57 ± 1.6 mg/dL; Cre, 0.52 ± 0.1 mg/dL). Collectively, serum level of BUN and Cre increased by cisplatin decreased by cyanroside administration in balb/c mice.

Cynaroside reduces cisplatin-induced nephrotoxicity in vivo model. Comparing the histological feature in different groups, the renal cortex of mice revealed a tubular histological structure using H&E staining (Fig. 5A). In cisplatin administrated mice (cisplatin group), histological examination revealed loss of brush border, and desquamation of epithelial cells in renal tubular epithelium. In contrast, degenerative changes such as loss of brush border markedly recovered by cynaroside administration (cisplatin + cynaroside group) in renal tissue. Cisplatin administration increased Tunel positive signal in renal tissue, in contrast, administration of cynaroside in cisplatin-injected mice reduced Tunel positive signal (Fig. 5B).

DISCUSSION

Pathogenesis of nephrotoxicity by cisplatin was associated with cell death and inflammation (16-18). Apoptotic cell death is an important process in cisplatin-induced nephrotoxicity, MST-1 involved in cell death of cancer cell line such as U2OS, HepG2, and HCT116 (19,20). Caspase-3 cleavage MST-1 occurs during apoptosis in mammalian cell (21-23). In recent years, use of natural medicines has developed to reduced cisplatin-induced nephrotoxicity (24-26). In this study, we demonstrated that cynaroside has a renoprotective effect on cisplatin-induced nephrotoxicity in mice kidneys, by attenuating degenerative changes such as less of brush border, desquamation of epithelial cells, and elevated BUN, Cre, and neutrophils in blood. Findings revealed that cisplatin-induced cell death in HK-2 cells was ameliorated by cynaroside treatment. Based on results, it was hypothesized that cynaroside treatment may be improved in cisplatin-induced nephrotoxicity. This hypothesis is supported by the following evidence: 1) Induction of caspase-3/MST-1 signaling, DNA fragmenta-

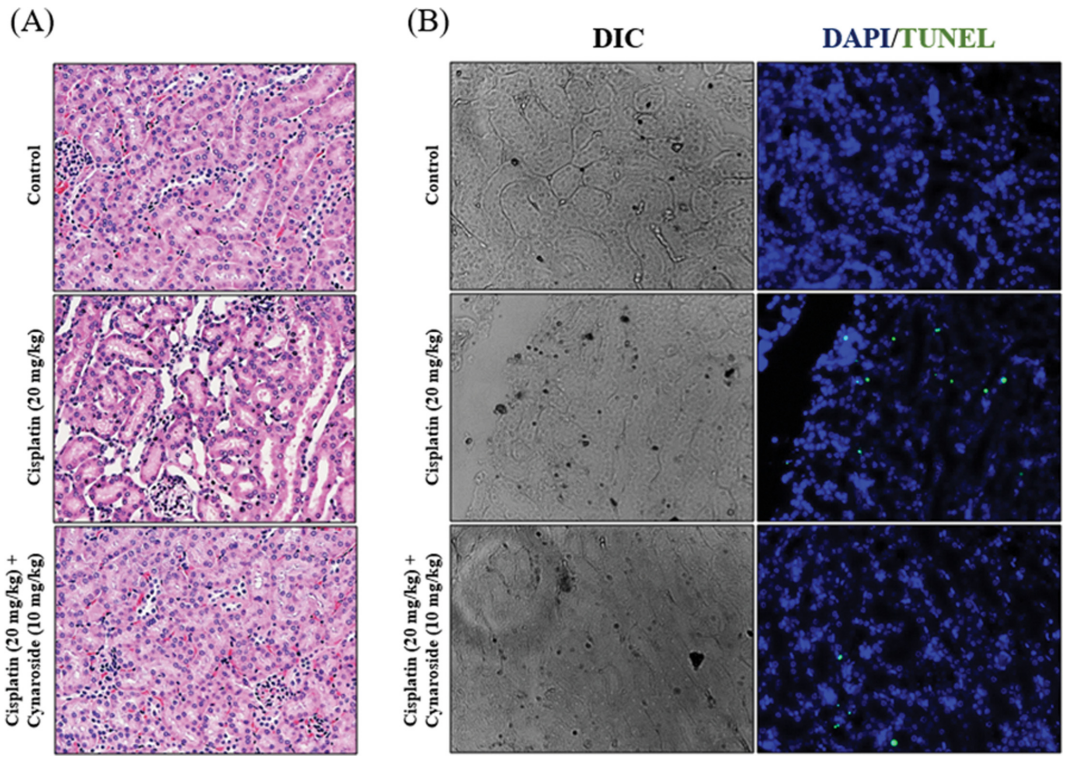

Fig. 5. Cynaroside reduces cisplatin-induced nephrotoxicity on animal model. (A-B) Mice were separated 3 group (Control; n = 7, Cisplatin (20 mg/kg); n = 7, Cisplatin (20 mg/kg) + Cynaroside (10 mg/kg); n = 7). Mice were administered with vehicle or cisplatin (20 mg/kg). Representative images were stained by hematoxylin and eosin (H&E) staining. Representative images are from at least three independent experiments.

tion, and mitochondrial dysfunction during apoptotic cell death was attenuated by cynaroside treatment *in vitro*, 2) Cisplatin-induced nephrotoxicity improved by cynaroside administration on *in vivo*.

Initially, we anticipated that cisplatin-induced DNA fragmentation during cell death was ameliorated by cynaroside treatment on HK-2 cells. DNA fragmentation was involved in cisplatin-induced nephrotoxicity, and was implicated in cisplatin administration *in vivo* (27,28). Cisplatin treatment in HK-2 cells induced DNA fragmentation, prevented by cynaroside treatment (Fig. 1B), and increased DNA fragmentation induced by cisplatin administration was diminished by cynaroside administration on mice (Fig. 5B). Apoptotic DNA fragmentation occurs during programmed cell death (apoptosis), and is a hallmark of apoptosis (29,30). Thus, cynaroside diminished cisplatin-induced DNA fragmentation during cell death. Next, we observed that apoptotic cell death rates (apopotosis + cell death on FACS analysis) and mitochondrial dysfunction were induced by cisplatin treatment on HK-2 cells. According to recent studies, mitochondrial dysfunction increased during apoptosis process (31). Mitochondrial membrane permeabilization may constitute apoptosis. Decrease in MMP (mitochondrial membrane potential) is a universal feature of apoptosis (32,33). This study confirmed measurement of apoptotic cell death (Fig. 2A) and MMP (Fig. 2B), rates of apoptotic cell death increased by cisplatin treatment, but is ameliorated by cynaroside pre-treatment (Fig. 2A). Decreased mitochondrial membrane potential induced by cisplatin recovered with pre-treatment of cynaroside on HK-2 cells (Fig. 2B), suggesting that cynaroside may be involved in mitochondria and apoptosis process inhibiting cisplatin-induced mitochondrial dysfunction and apoptotic cell death. As previously mentioned, MST-1 is involved in cell death, and its activation requires autophosphorylation at Thr^{183} and Thr^{187} and caspase-3 mediated cleavage leading to initiation of DNA fragmentation and chromatin condensation (11-13). Thus, we observed caspase-3/MST-1 signaling pathway under cisplatin-induced cell death in HK-2 cells, cisplatin treatment increased protein expression and cleaved form of MST-1, caspase-3, and autophosphorylation of MST-1 at Thr^{183} and Thr^{187}, but which are diminished with pre-treatment of cynaroside (Fig. 3A). Caspase-3 activation induced by cisplatin treatment decreased by cyanroside (Fig. 3B). Yuna, et al. reported that cisplatin-induced cell death in HCT116 a human colorectal cancer cell line, it promoted by apoptosis via MST-1 in a p53-dependent manner (19). Results indicated that, MST-1 and caspase-3 induced by cisplatin treatment were involved in cisplatin-induced cell death in HK-2 cells. According to many reports, cisplatin-induced nephrotoxicity was associated with inflammation such as neutrophil infiltration and secretion of cytokines (16,34), and cisplatin administration increased creatinine (Cre) and blood urea nitrogen (BUN) in serum (35). Thus, we observed neutrophil, Cre, and BUN in blood. Neutrophil, BUN, and Cre in blood increased by cisplatin administration, and decreased by cyanroside administration (Fig. 5A, 5B).

Cisplatin administration increased tubular damage and DNA fragmentation in kidneys, ameliorated by cynaroside administration. Park *et al*. (36) reported that cynaroside inhibited lipopolysaccharide-stimulated inflammatory response through NF-κB. Cynaroside has anti-cancer effect on human liver cancer cells (37), and has protective effect against doxorubicin-induced injury through PTEN/Akt and ERK pathway in H9c2 cells a rat myoblast (38). Evidence supports these results, and suggests that cynaroside may be recovered cisplatin-induced nephrotoxicity via inhibiting caspase-3/MST-1 signaling pathway. In conclusion, this study found that cynaroside decreased cisplatin-induced cell death though inhibiting caspase-3/MST-1 signaling pathway in HK-2 cells, and was attenuated cisplation-induced nephrotoxicity and the elevated neutrophil, BUN, and Cre in blood. Collectively, findings suggest that cynarorside could be used to for improving cisplatin-induced side effects. However, further experiments are required regarding toxicity by high dose cynaroside and caspase-3/MST-1 signaling pathway *in vivo*.

ACKNOWLDGMENTS

This study was supported by the Korean Medicinal Herb-based Business of the Korean Traditional Resource, Ministry of Health and Welfare, Republic of Korea.

Received November 8, 2017; Revised March 12, 2018; Accepted March 13, 2018

REFERENCES

1. Park, J.C., Park, J.G., Kim, H.J., Hur, J.M., Lee, J.H., Sung, N.J., Chung, S.K. and Choi, J.W. (2002) Effects of extract from Angelica keiskei and its component, cynaroside, on the hepatic bromobenzene-metabolizing enzyme system in rats. *Phytother. Res*., **16**, S24-S27.
2. Sun, X., Sun, S.G., Wang, M., Xiao, J. and Sun, X.B. (2011) Protective effects of cynaroside against H2O2-induced apoptosis in H9c2 cardiomyoblasts. *J. Cell Biochem.*, **112**, 2019-2029.
3. Wen, H.U., Ting, G., Jiang, W.J., Dong, G.L., Chen, D.W., Yang, S.L. and Li, H.R. (2015) Effects of ultrahigh pressure extraction on yield and antioxidant activity of chlorogenic acid and cynaroside extracted from flowe bubs of *Lonicera japonica*. *Chin. J. Nat. Med*., **13**, 445-453.
4. Lin, L.C., Pai, Y.F. and Tsai, T.H. (2015) Isolation of luteolin and luteolin-7-O-glucoside from Dendranthema morifolium Ramat Tzvel and pharmacokinetics in rat. *J. Agric. Food Chem*., **9**, 7700-7706.
5. Kang, K.J. and Lee, J.H. (2010) Characteristics of gastric

cancer in Korea-with an emphasis on the increase of the early gastric cancer (EGC). *J. Korean Med. Assoc*., **53**, 283-289.
6. Kang, K.P., Kim, D.H., Jung, Y.J., Lee, A.S., Lee, S., Lee, S.Y., Jang, K.Y., Sung, M.J., Park, S.K. and Kim W. (2009) Alpha-lipoic acid attenuates cisplatin-induced acute kidney injury in mice by suppressing renal inflammation. *Nephrol. Dial. Transplant*., **24**, 3012-3020.
7. Kolb, R., Ghazi, M. and Barfuss, D. (2003) Inhibition of basolateral transport and cellular accumulation of cDDP and N-acetyl-L-cysteine-cDDP by TEA and PAH in the renal proximal tubule. *Cancer. Chemother. Pharmacol*., **51**, 132-138.
8. Ronald, P.M., Raghu. K.T., Ganesan, R. and William, B.R. (2010) Mechanisms of cisplatin nephrotoxicity. *Toxins (Basel)*, **2**, 2490-2518.
9. Yao, X., Panichpisal, K., Kurtzman, M. and Nugent, K. (2007) Cisplatin nephrotoxicity: a review. *Am. J. Med. Sci*., **334**, 115-154.
10. Ling, P., Lu, T.J., Yuan, C.J. and Lai, M.D. (2008) Biosignaling of mammalian Ste20-related kinases. *Cell. Signal*., **20**, 1237-1247.
11. Qin, F., Tian, J., Zhou, D. and Chen, L. (2013) Mst1 and Mst2 kinases: regulations and disease. *Cell. Biosci*., **3**, 31.
12. Meng, Z., Moroishi, T. and Guan, K.L. (2016) Mechanisms of hippo pathway regulation. *Genes Dev*., **30**, 1-17.
13. Amin, A., Federico, P., Zahra, A., Supreet, K., Vrushali, K., Ting, Y., Thomas, F., Wufan, T., Jose, O., Francois, P., Julie, K.C. and Kathrin, M. (2014) MST-1 is a novel regulator of apoptosis in pancreatic beta-cells. *Nat. Med*., **20**, 385-397.
14. Caretha, L.C. and Jonathan, C. (1995) Cloning and characterization of a human protein kinase with homology to Ste20. *J. Biol. Chem*., **270**, 21695-21700.
15. Parham, M., Inti, Z., Kristi, B., Luigi, T., Luigi, T., Jeremy, R.J. and Alessandro, L. (2007) Prognostic significance of mammalian sterile20-like kinase 1 in colorectal cancer. *Mod. Pathol*., **20**, 331-338.
16. Faunel, S., Lewis, E.C., Reznikov, L., Koke, T.S., Somerset, H., Oh, D.J., Li, L., Klein, C.L., Dinarello, C.A. and Edelstein, C.L. (2007) Cisplatin-induced acute renal failure is associated with an increase in the cytokines interleukin (IL)-1beta, IL-18, IL-6, and neutrophil infiltration in the kidney. *J. Phamacol. Exp. Ther*., **322**, 8-15.
17. Ozkok, A. and Edelstein, C.L. (2014) Pathophysiology of cisplatin-induced acute kidney injury. *Biomed. Res. Int*., **2014**, 967826.
18. Oh, G.S., Kim, H.J., Shen, A.H., Lee, S.B., Khadka, D., Pandit, A. and So, H.S. (2014) Cisplatin-induced kidney dysfunction and perspectives on improving treatment strategies. *Electrolyte Blood Press*, **12**, 55-65.
19. Yuna, F., Xie, Q., Wu, J., Bai, Y., Mao, B., Dong, Y., Bi, W., Ji, G., Tao, W., Wang, Y. and Yuan, Z. (2011) MST-1 promotes apoptosis through regulating sirt1-dependent p53 deacetylation. *J. Biol. Chem*., **286**, 6940-6945.
20. Xu, C., Liu, C., Huang, W., Tu, S. and Wan, F. (2013) Effect of mst1 overexpression on the growth of human hepatocellular carcinoma HepG2 cells and the sensitivity to cisplatin *in vitro*. *Acta Biochim. Biophys. Sin. (Shanghai)*, **45**, 268-279.
21. Ura, S., Masuyama, M., Graves, J.D. and Gotoh, Y. (2001) MST1-JNK promotes apoptosis via caspase-dependent and independent pathways. *Genes Cells*, **6**, 519-530.
22. Maejima, Y., Kyoi, S., Zhai, P., Liu, T., Li, H., Lvessa, A., Sciarretta, S., Del Re, D.P., Zablocki, D.K., Hsu, C.P., Lim, D.S., Isobe, M. and Sadoshima, J. (2013) Mst1 inhibits autophagy by promoting the interaction between Beclin1 and Bcl-2. *Nat. Med*., **19**, 1478-1488.
23. Luo, X., Li, Z., Yan, Q., Li, X., Tao, D., Wang, J., Leng, Y., Gardner, K., Judge, S., Li, Q., Hu, J. and Gong, J. (2010) The human WW45 protein enhances MST-1 mediated apoptosis *in vivo*. *Int. J. Mol. Med*., **23**, 357-362.
24. Hosseinian, S., Rad, A.K., Hadjzadeh, M.A.R., Roshan, N.M., Havakhah, S. and Shafiee, S. (2016) The protective effect of *Nigella sativa* against cisplatin-induced nephrotoxicity in rats. *Avicenna J. Phytomed*., **6**, 44-54.
25. Bami, E., Ozakpinar, O.B., Ozdemir-Kumral, Z.N., Koroglu, K., Ercan, F., Cirakli, Z., Sekerler, T., Izzettin, F.V., Sancar, M. and Okuyan, B. (2017) Protective effect of ferulic acid on cisplatin induced nephrotoxicity in rats. *Environ. Toxicol. Pharmacol*., **54**, 105-111.
26. Lou, X.Y., Cheng, J.L. and Zhang, B. (2015) Therapeutic effect and mechanism of breviscapine on cisplatin-induced nephrotoxicity in mice. *Asian. Pac. J. Trop. Med*., **8**, 873-877.
27. Yin, X., Apostolov, E.O., Shah, S.V., Wang, X., Bogdanov, K.V., Buzder, T., Stewart, A.G. and Basnakian, A.G. (2007) Induction of renal endonuclease G by cisplatin is reduced in DNase I-deficient mice. *J. Am. Soc. Nephrol*., **18**, 2544-2553.
28. Basnakian, A.G., Apostolov, E.O., Yin, X., Napirei, M., Mannherz, H.G. and Shah, S.V. (2005) Cisplatin nephrotoxicity is mediated by deoxyribonuclease I. *J. Am. Soc. Nephrol*., **16**, 697-702.
29. Hua, Z.J. and Xu, M. (2000) DNA fragmentation in apoptosis. *Cell Res*., **10**, 205-211.
30. Khodarev, N.N., Sokolova, I.A. and Vaughan, A.T. (1998) Mechanisms of induction of apoptotic DNA fragmentation. *Int. J. Radiat. Biol*., **73**, 455-467.
31. Jang, Y.J., Won, J.H., Back, M.J., Fu, Z., Jang, J.M., Ha, H.C., Hong, S.B., Chang, M. and Kim, D.K. (2017) Paraquat induces apoptosis through a mitochondria-dependent pathway in RAW 264.7 cells. *Biomol. Ther. (Seoul)*, **23**, 407-413.
32. Kroemer, G. and Reed, J.C. (2000) Mitochondrial control of cell death. *Nat. Med*., **6**, 513-519.
33. Wadia, J.S., Chalmers-Redman, R.M.E., Ju, W.J.H., Carlile, G.W., Philips, J.L., Fraser, A,D. and Tatton, W.G. (1998) Mitochondrial membrane potential and nuclear changes in apoptosis acused by serum and nerve growth factor withdrawal: time course and modification by (-)-deprenyl. *J. Neurosci*., **18**, 932-947.
34. Tadagavadi, R. and Reeves, W.B. (2017) Neutrophils in cisplatin AKI-mediator or marker? *Kidney Int*., **92**, 11-13.
35. Ma, P., Zhang, S., Su, G., Qiu, G. and Wu, Z. (2015) Protective effects of icariin on cisplatin-induced acute renal injury in mice. *Am. J. Transl. Res*., **7**, 2105-2114.
36. Park, C.M. and Song, Y.S. (2013) Luteolin and luteolin-7-*O*-glucoside inhibit lipopolysaccharide-induced inflammatory responses through modulation of NF-κB/AP-1/PI3K-Akt

signaling cascades in RAW 264.7 cells. *Nutr. Res. Pract.*, **7**, 423-429.
37. Hwang, Y.J., Lee, E.J., Kim, H.R. and Hwang, K.A. (2013) Molecular mechanisms of luteolin-7-O-glucoside-induced growth inhibition on human liver cancer cells: G2/M cell cycle arrest and caspase-independent apoptotic signaling pathways. *BMB Rep.*, **46**, 611-616.
38. Yao, H., Shang, Z., Wang, P., Li, S., Zhang, Q., Tian, H., Ren, D. and Han, X. (2016) Protection of luteolin-7-O-glucoside against doxorubicin-induced injury through PTEN/Akt and ERK pathway in H9c2 cells. *Cardiovasc. Toxicol.*, **16**, 101-110.